IET Electric Power Applications

Research Article

IET Journals
The Institution of Engineering and Technology

Theory of symmetric winding distributions and a general method for winding MMF harmonic analysis

ISSN 1751-8660
Received on 30th June 2020
Revised 30th September 2020
Accepted on 13th October 2020
E-First on 26th January 2021
doi: 10.1049/iet-epa.2020.0553
www.ietdl.org

Yi Sun[1,2], Yingqian Lin[1,2], Yunchong Wang[1,2], Robert Nilssen[1,3], Jian-Xin Shen[1,2] ✉

[1]*College of Electrical Engineering, Zhejiang University, Hangzhou, People's Republic of China*
[2]*Zhejiang Provincial Key Laboratory of Electrical Machine Systems, Hangzhou, People's Republic of China*
[3]*Department of Electric Power Engineering, Norwegian University of Science and Technology, Trondheim, Norway*
✉ *E-mail: J_X_Shen@zju.edu.cn*

Abstract: One of the main challenges in motor design is the winding layout, including winding distributions and magnetomotive force (MMF) harmonic analysis. Considering some shortcomings in the existing theories for winding distributions and difficulties in dealing with unconventional fractional-slot windings, a unified theory of symmetric winding distributions is proposed. First, this study gives the sufficient and necessary conditions for a *m*-phase symmetric winding and the novel winding distribution formula. Subsequently, a general method for MMF harmonic analysis including the amplitude of MMF harmonics and harmonic orders are proposed. Finally, the analysis results show that this unified theory is an efficient and compact method to deal with the winding layout to analyse all kinds of winding MMF harmonics.

1 Introduction

Winding design plays an important role in the whole process of motor design. There are a lot of classification standards for all types of windings [1]. According to the slot per-pole per-phase being an integer or not, windings can be divided into integer-slot and fractional-slot windings. The integer-slot distributed windings (ISDWs) have been widely used in most categories of AC machines such as the regular induction and synchronous machines, as well as many special-structure machines, e.g. the vernier machines, flux reversal machines etc. In general, the ISDWs have the merits of low space magnetomotive force (MMF) harmonics and simple structure, though sometimes they are designed to be rather complex so as to achieve better motor performance, such as lower space harmonics or torque ripple. On the other hand, the fractional-slot concentrated windings (FSCWs) have shorter end-windings [2, 3] than the ISDWs, resulting in less copper material usage and less ohmic loss. Furthermore, the FSCWs structure often enhances the winding fault tolerance [4, 5] and reduces the cogging torque in permanent magnet machines [6], but usually causes high space MMF harmonics [7, 8].

After the selection of the number of phases as m, the number of slots as Q, and the number of pole pairs as p, the subsequent work is normally to finish the winding layout. The classical theory of the star of slots [9] can handle many complicated windings and the whole process of distributing the winding is a graphical display. However, for an arbitrary winding with m-phase, the number of slots is Q and pole pairs is p, this theory cannot qualify the feasibility of winding distributions directly. Moreover, for some windings with large number of slots or multiphase windings, it is a labourious and time-consuming process. Thus, this classical theory is not satisfactory for automatic winding procedures implemented in a computer program. An improved fractional-slot theory has been proposed in [10, 11]. This theory can handle two such types of windings well:

- Double-layer windings with an odd-phase number and a constant coil pitch.
- Single-layer windings with an odd-phase number and a constant odd coil pitch.

However, for windings with the even phases, single-layer windings with a non-constant coil pitch, and some asymmetrical multiphase windings, this feasibility theory is not suitable anymore.

In this paper, a unified theory for symmetric winding distributions is proposed. First, the sufficient and necessary conditions of m-phase symmetric winding distributions are presented. Then, a novel winding distribution formula, which can provide a fast automatic winding distributions algorithm is established. It is noteworthy that some asymmetrical windings such as a dual three-phase asymmetrical winding with 12-slot/10-pole combination [12] and a dual five-phase asymmetrical winding with 20-slot/18-pole combination [13], can be converted to symmetric windings by the procedure described in this paper. These windings can then be handled well by the theory of symmetric winding distributions.

After finishing the winding distribution, it is necessary to calculate the winding MMF. It is well known that the winding MMF has a great influence on torque ripple [14, 15], rotor eddy-current losses [16–18] and undesirable noise sometimes accompanied by vibrations [19, 20]. MMF calculations have been presented many times in the literatures. For example, in [10, 11], the star of slots is used to determine the order of MMF harmonics qualitatively and to calculate the winding factors for some winding types. In [21], parameters of four, five, and six-phase FSCWs, including the winding factors and MMF harmonics for each slot/pole combinations are calculated. In [22], a new non-overlapping winding topology is proposed, which can reduce the MMF harmonics more effectively than the FSCWs. However, these works are mainly researched on some specific winding types or to obtain some qualitative conclusions. Thus, in this paper, a general MMF calculation method for all windings will be presented and the MMF calculation results can be used generally for electrical machine design.

2 Theory of symmetric winding distributions

First, the symmetry of winding is given by the following:

- Q slots uniformly distributed on the stator.
- p pole pairs permanent magnets uniformly distributed on the rotor.

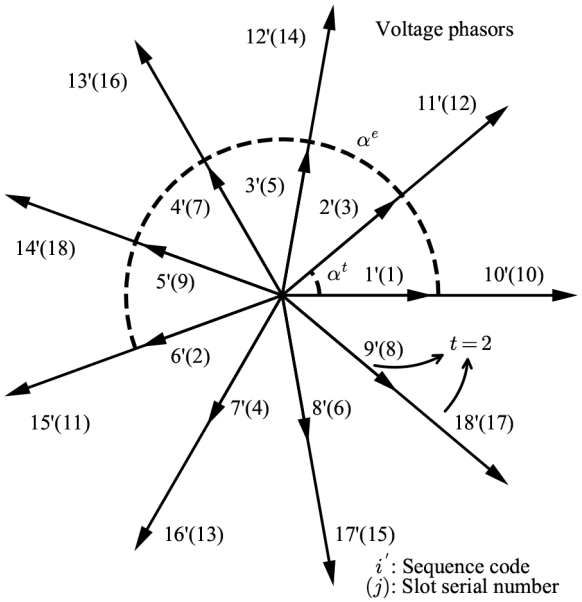

Fig. 1 *Distribution of upper-side voltage phasors for the double-layer winding with* $Q = 18$, $2p = 20$ *and* $t = 2$

Subsequently, it is necessary to define phase bands, the number of phases as m, winding types, the coil pitch as y_q, and the symmetric winding feasibility.

Regarding phase bands and the number of phases as m, each phase of a certain symmetric winding consists of two phase bands, the positive phase band being $[\theta_0, \theta_0 + (\pi/m))$ and the negative phase band being $[\theta_0 + \pi, \theta_0 + (\pi/m) + \pi)$. Then, the number of phases of this winding is m.

Regarding winding types, there are many different classification standards. In this paper, windings will be divided into the single-layer and double-layer windings based on the number of coil sides per slot. For a coil, one coil side is called as the upper side, and the other is called as the lower side in the following sections.

The coil pitch y_q can be defined by:

$$y_q^j = L^j - U^j + kQ, \quad 1 \le y_q^j < Q \tag{1}$$

where y_q^j is the jth coil pitch and the value of y_q^j can be generally selected as an integral part of $Q/2p$, then L^j is the lower-side slot serial number of the jth coil, U^j is the upper-side slot serial number of the jth coil, Q is the number of slots, and k is an integer.

Symmetric winding feasibility is fully based on the basic principle of winding distribution [10], which obtains the following conditions:

- Maximise fundamental electromotive force (EMF).
- The EMF waveform of each phase is equal.
- The electrical angle between fundamental EMF phasors of the jth phase and the $(j + 1)$th phase is constant. Here $1 \le j < m$.

Here the fundamental EMF in the coils is induced by the sinusoidal rotating magnetic field with $2\pi/p$ wavelength on the rotor.

The first point is satisfied by using positive and negative phase bands. To satisfy the second and last points, the number of coils Q/m in each phase must be the same.

Before obtaining the sufficient and necessary conditions of the symmetric winding feasibility, it is necessary to investigate the distribution law of the fundamental coil voltage phasors.

2.1 Uniformity and periodicity in the distribution of fundamental upper-side voltage phasors

First, a double-layer winding is investigated with the number of slots Q, pole pairs p and a constant coil pitch y_q. The distribution of upper-side voltage phasors is the same as that of coil voltage phasors, which are due to the constant coil pitch y_q.

For this double-layer winding, there are Q upper sides in total. Phase angles of fundamental upper-side voltage phasors can be included in the following set U:

$$\{0, \alpha^e, 2\alpha^e, \ldots, (Q-1)\alpha^e\}$$

where α^e is electrical slot angle, $\alpha^e = 2\pi p/Q$, and each subscript of elements in U is the corresponding slot serial number.

Then, map the set U to the set V, $U \xrightarrow{e^{j(\cdot)}} V$:

$$\{1, e^{j\alpha^e}, e^{j2\alpha^e}, \ldots, e^{j(Q-1)\alpha^e}\}$$

It is noted that there might be duplicate elements in the set V. It can be strictly proven that the number of independent elements is Q/t, where t is the number of basic windings [10], $t = \mathrm{GCD}(Q, p)$.

According to the following equation:

$$e^{jk\alpha^e} = e^{j(k + n(Q/t))\alpha^e}$$

where k and n are integers.

Therefore, the set V is fully equivalent to the set V'

$$\{1, e^{j\alpha^e}, e^{j2\alpha^e}, \ldots, e^{j((Q/t)-1)\alpha^e}\}$$

Then, a new set W can be constructed:

$$\{1, e^{j\alpha^t}, e^{j2\alpha^t}, \ldots, e^{j((Q/t)-1)\alpha^t}\}$$

where $\alpha^t = 2\pi t/Q$.

It can be seen that the number of elements in both V' and W is Q/t. The jth element in V' can be represented by the i'th element in W, which is shown as

$$j = \left(i' - 1 + k\frac{Q}{t}\right)\frac{t}{p} + 1 \tag{2}$$

where $1 \le i' \le Q/t$, $1 \le j \le Q/t$, and k is an integer.

It should be noted that the number j represents the slot serial number and the number i' is called as the sequence code in this paper. Thus, the winding distribution formula (2) establishes the relationship between the sequence code and the slot serial number.

According to (2), it can be seen that elements in V' and elements in W are corresponding one by one and there are Q/t independent elements in both sets. Therefore, two important conclusions can be drawn as follows:

- *Uniformity*: The first Q/t upper-side voltage phasors are uniformly distributed and the angle between two adjacent voltage phasors is α^t.
- *Periodicity*: The voltage phasor of the jth upper side is exactly the same as that of the $(j + k(Q/t))$th one, here k is an integer.

For a more intuitive comparison of electrical angle α^e and the angle α^t between two adjacent voltage phasors, an example with $Q = 18$, $2p = 20$, and $t = 2$ is shown in Fig. 1.

2.2 Sufficient and necessary conditions of m-phase symmetric winding distributions

According to Section 2.1, upper-side voltage phasors of a double-layer winding are periodically distributed. Therefore, only the first cycle of upper-side voltage phasors need to be concerned. Thanks to the winding distribution formula (2), only the sequence code needs to be concerned in this subsection.

2.2.1 m-phase double-layer windings with the number of slots Q, pole-pairs p, and a constant coil pitch: According to the symmetric winding feasibility, the number of coils Q/m in each

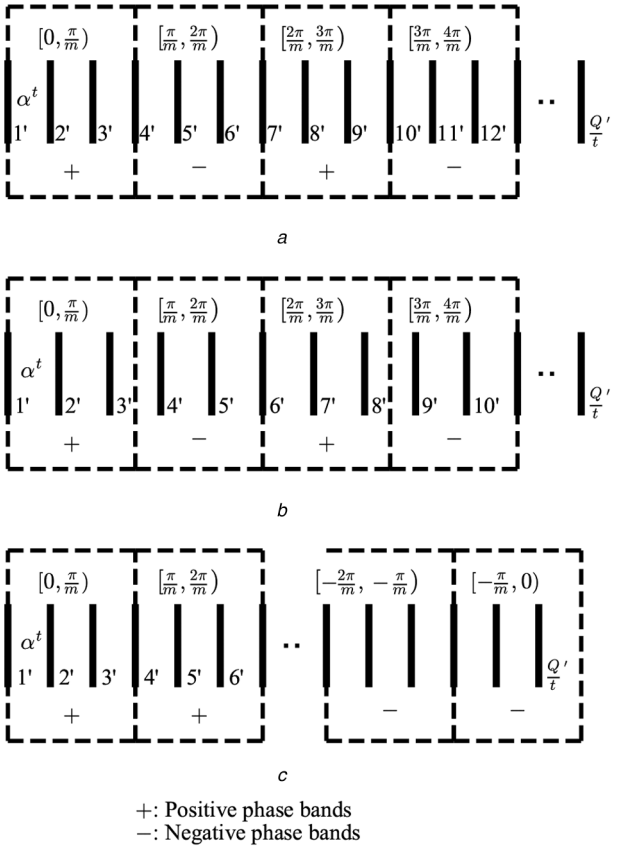

Fig. 2 *Relative positional relationship between phase bands and voltage phasors*
(a) m = odd, Q/mt = even, ***(b)*** m = odd, Q/mt = odd, ***(c)*** m = even, Q/mt = even

phase must be the same and an integer. Considering the periodicity in the distribution of voltage phasors Q/mt must be an integer as a basic necessary condition.

Then, the relative positional relationship between phase bands and voltage phasors needs to be investigated. The position of the kth phase band $[(k-1)\pi/m, k\pi/m)$ can be expressed as:

$$\frac{(k-1)\pi}{m\alpha^t} = \frac{Q}{mt}\cdot\frac{(k-1)}{2}, \quad \frac{k\pi}{m\alpha^t} = \frac{Q}{mt}\cdot\frac{k}{2} \tag{3}$$

where $1 \le k \le 2m$.

According to (3), both the front and back edges of the kth phase band overlap voltage phasors when Q/mt is even, which is shown in Fig. 2*a*. When Q/mt is odd, one edge overlaps one voltage phasor, and the other edge locates at the middle of two voltage phasors, which is shown in Fig. 2*b*.

For the distribution of phase bands, there are two types:

(a) The distribution of phase bands is positive and negative alternatively.
(b) The first half are all positive phase bands and the latter half are all negative phase bands.

When the number of phases m is odd, take the (a) type, which is shown in Figs. 2*a* and *b*. Then, assume that there are a voltage phasors in a certain positive phase band and b in the negative one per cycle. The simple relationship among a, b, and Q/mt can be drawn as:

$$a+b = \frac{2\pi}{m\alpha^t} = \frac{Q}{mt}\begin{cases} a=b & \dfrac{Q}{mt} = \text{even} \\ a=b+1 & \dfrac{Q}{mt} = \text{odd} \end{cases} \tag{4}$$

In this case, when Q/mt is an integer, the distribution of voltage phasors of each phase is exactly the same. Thus, this double-layer winding satisfies the requirement of symmetric winding feasibility and the electrical angle between fundamental EMF phasors of two adjacent phases is $2\pi/m$.

When m is even, suppose the jth phase band belongs to one positive phase, the $(j+m)$th phase band must belong to its negative one. If using the (a) type, all odd-numbered phase bands are positive phase bands. Let $j=1$, then $1+m$ is odd and the $(1+m)$th phase band belongs to positive and negative phase bands at the same time. In this case, the negative phase band of a certain phase will overlap the positive phase band of another phase. Thus, use the (b) type, which is shown in Fig. 2*c*, assuming that there are a voltage phasors in one phase band and b in the adjacent one per cycle. To satisfy the requirement of symmetric winding feasibility, the simple relationship among a, b, and Q/mt can be drawn as:

$$a = b = \frac{Q}{2mt} \tag{5}$$

In this case, the sufficient and necessary conditions of winding feasibility for double-layer windings with a constant coil pitch are that $Q/2mt$ is an integer. Moreover, the electrical angle between fundamental EMF phasors of the jth phase and the $(j+1)$th phase is π/m. Here $1 \le j < m$.

2.2.2 m-phase single-layer windings with the even number of slots Q and pole-pairs p: For a single-layer winding, there are $Q/2$ upper sides and Q must be even. There are two methods dealing with single-layer winding distribution:

- Let the coil pitch be constant and odd. Then, remove all lower sides. Finally, convert a single-layer winding to a double-layer winding.
- According to the distribution law of voltage phasors, let all coil sides be divided into upper and lower sides directly.

For the first one, when the coil pitch is odd, all lower sides are in even-numbered slots and all upper sides are in odd-numbered slots. Moreover, all upper sides are still uniformly distributed on the stator. Thus, this single-layer winding can be converted to the equivalent double-layer winding with m-phase, the number of slots $Q/2$, pole pairs p, and a constant odd coil pitch y_q. Then, the key point is to calculate the number of basic windings t'.

When m is odd:

- Let Q/t be even and $t = \mathrm{GCD}(Q, p)$, the number of basic windings t' can be calculated by:

$$t' = \mathrm{GCD}\left(\frac{Q}{2}, p\right) = \mathrm{GCD}\left(\frac{Q}{2t}\cdot t, \frac{p}{t}\cdot t\right) = t \tag{6}$$

  Thus, according to the previous analysis, the sufficient and necessary conditions are that $Q/2mt$ is an integer and Q is even. Since Q/t is even and m is odd, Q/mt must be even as long as Q/mt is an integer. Therefore, the sufficient and necessary conditions can be concluded that Q/mt is an integer and Q is even.
- Let Q/t be odd, then t must be even. The number of basic windings t' can be calculated by:

$$t' = \mathrm{GCD}\left(\frac{Q}{2}, p\right) = \mathrm{GCD}\left(\frac{Q}{t}\cdot\frac{t}{2}, \frac{2p}{t}\cdot\frac{t}{2}\right) = \frac{t}{2} \tag{7}$$

Thus, the sufficient and necessary conditions are that Q/mt is an integer and Q is even.

In summary, when m is odd, the sufficient and necessary conditions of winding feasibility for single-layer windings with a constant odd coil pitch are that Q/mt is an integer and Q is even.

When m is even, assume that Q/t is odd, according to (7), $t' = t/2$. Thus, the sufficient and necessary conditions of winding feasibility for this equivalent double-layer windings are that $Q/2mt$ is an integer, which apparently contradicts the hypothesis. In this case, Q/t must be even. Then, according to (6), $t' = t$. Thus, the

Table 1 Sufficient and necessary conditions of m-phase symmetric winding distributions

Winding type[a]	Preconditions			Sufficient and necessary conditions
	m-phase	Phase angle[b]	Coil pitch y_q	
double layer	odd	$\frac{2\pi}{m}$	constant	$\frac{Q}{mt} = \text{integer}$
	even	$\frac{\pi}{m}$		$\frac{Q}{2mt} = \text{integer}$
single layer	odd	$\frac{2\pi}{m}$	constant and odd	$\frac{Q}{mt} = \text{integer}$ and $Q = \text{even}$
	even	$\frac{\pi}{m}$		$\frac{Q}{4mt} = \text{integer}$
	when the corresponding double-layer winding is feasible			$Q = \text{even}$

[a]Winding type property: symmetry, m-phase, phase band width π/m, the number of slots Q, pole pairs p, and the number of basic windings $t = \text{GCD}(Q, p)$.

[b]Phase angle refers to the electrical angle between fundamental EMF phasors of the jth phase and the $(j + 1)$th phase. Here $1 \leq j < m$.

Table 2 Winding configurations of four models

Models	4p18s-DL	22p20s-DL	22p24s-SL	4p18s-SL
number of phases m	3	5	6	3
number of slots Q	18	20	24	18
number of poles $2p$	4	22	22	4
number of basic windings t	2	1	1	1
coil pitch y_q	4	1	1	3, 4
winding type	double layer	double layer	single layer	single layer

Table 3 Double-layer winding with $m = 3$, $Q = 18$, $2p = 4$

Phase bands	$A+$	$C-$	$B+$	$A-$	$C+$	$B-$
sequence code	$(1', 2')$	$(3')$	$(4', 5')$	$(6')$	$(7', 8')$	$(9')$
slot serial number[a]	(1, 2)	(3)	(4, 5)	(6)	(7, 8)	(9)
—	(10, 11)	(12)	(13, 14)	(15)	(16, 17)	(18)

[a]Slot serial number represents the upper-side position.

sufficient and necessary conditions of winding feasibility for single-layer windings with a constant odd coil pitch are that $Q/4mt$ is an integer.

For the second one, first, it is assumed that the corresponding double-layer winding with a constant coil pitch is feasible. For this corresponding double-layer winding, there are $a \cdot t$ upper-side voltage phasors in a certain positive phase and $b \cdot t$ upper-side voltage phasors in the negative one when considering all t cycles. Thus, the key task is to let these coil sides, which correspond to these voltage phasors, be divided into upper sides and lower sides. According to (4), there are only two cases, $a = b$ or $a = b + 1$.

When $a = b$, using the phase A as an example, all coil sides in $A+$ are upper sides and all in $A-$ are lower sides in every cycle. These upper and lower sides can correspond one by one and these coil sides belong to the phase A. It is worth pointing out that the common integer-slot single-layer winding such as $m = 3$, $Q = 24$, $2p = 4$, and $y_q = 6$ belongs to this case.

When $a = b + 1$, m must be odd. According to (4), Q/mt is odd. Since Q is even, t must be even. Then, this single-layer winding distributions can be divided into two steps:

- Take the phase A as an example, let all coil sides in $A+$ except the first one be upper sides and all in $A-$ be lower sides in every cycle. Thus, these upper and lower sides can correspond one by one and these coil sides belong to the phase A.
- Each positive phase has remaining t coil sides, which voltage phasors are exactly the same. Let $t/2$ coil sides in $A+$ be upper sides and $t/2$ coil sides in $B+$ be lower sides. These $t/2$ coil sides belong to the phase A. Then, let $t/2$ remaining coil sides in $B+$ be upper sides and $t/2$ coil sides in $C+$ be lower sides. These $t/2$ coil sides belong to the phase B. Repeat the above processes. Finally, let $t/2$ remaining coil sides in $M+$ be upper sides and $t/2$ remaining coil sides in $A+$ be lower sides. These $t/2$ coil sides belong to the phase M.

In summary, when the m-phase double-layer windings with a constant coil pitch are feasible, the sufficient and necessary conditions of winding feasibility for the corresponding single-layer windings are that Q is even.

2.3 Summary and examples

According to the previous analysis, the sufficient and necessary conditions of m-phase symmetric winding distributions are included in Table 1.

To get a more intuitive understanding of the theory of symmetric winding distributions, four typical examples are shown in Table 2.

For the 4p18s-DL, the number of basic windings $t = 2$ and the number of coils in each phase per cycle $Q/mt = 3$. Thus, this double-layer winding can be feasible according to Table 1. Then, according to (4), there are two upper-side voltage phasors in each positive band and one in each negative one per cycle. Then, the phase-band order of $m = 3$ is $A+$, $C-$, $B+$, $A-$, $C+$, $B-$. Thus, the sequence code i' can be drawn as presented in Table 3.

Then, the sequence code can be converted to the slot serial number by (2). In this case:

$$j = i'$$

where $t = p$ and k takes zero.

Thus, the slot serial number is exactly the same as the sequence code when $t = p$. Then, the slot serial number in the second cycle can be obtained by those in the first cycle plus Q/t. For other cycles, repeat the above process.

Finally, according to the coil pitch $y_q = 4$, the lower-side position can be determined. Thus, the whole winding distribution is complete and the diagram of this winding distribution is shown in Fig. 3*a*.

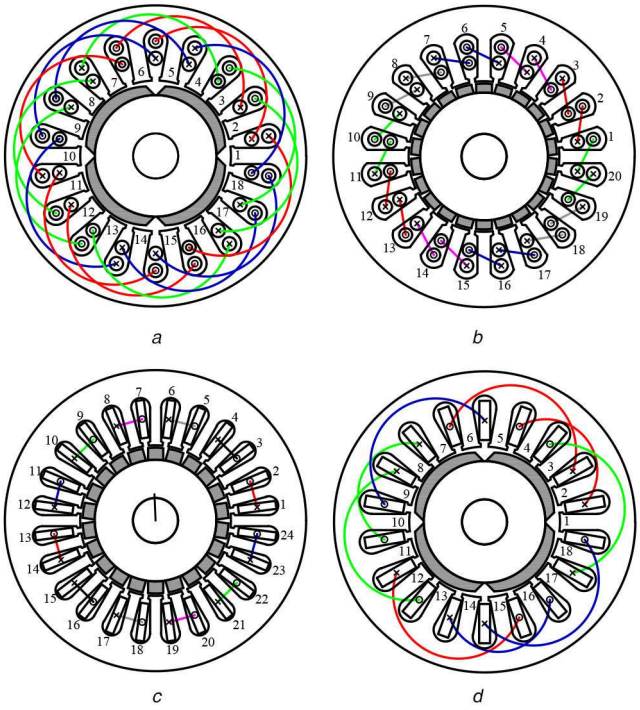

Fig. 3 *Diagram of winding distributions*
(a) 4p18s-DL, ***(b)*** 22p20s-DL, ***(c)*** 22p24s-SL, ***(d)*** 4p18s-SL

Table 4 Double-layer winding with $m = 5$, $Q = 20$, $2p = 22$

Phase bands	$A+$	$D-$	$B+$	$E-$
sequence code	$(1', 2')$	$(3', 4')$	$(5', 6')$	$(7', 8')$
slot serial number[a]	(1, 12)	(3, 14)	(5, 16)	(7, 18)
phase bands	$C+$	$A-$	$D+$	$B-$
sequence code	$(9', 10')$	$(11', 12')$	$(13', 14')$	$(15', 16')$
slot serial number	(9, 20)	(11, 2)	(13, 4)	(15, 6)
phase bands	$E+$	$C-$		
sequence code	$(17', 18')$	$(19', 20')$		
slot serial number	(17, 8)	(19, 10)		

[a]Slot serial number represents the upper-side position.

Table 5 Single-layer winding with $m = 6$, $Q = 24$, $2p = 22$

Phase bands	$A+$	$B+$	$C+$	$D+$
sequence code	$(1', 2')$	$(3', 4')$	$(5', 6')$	$(7', 8')$
slot serial number[a]	$(1, \not{1}2)$	$(23, \not{1}0)$	$(21, \not{8})$	$(19, \not{6})$
phase bands	$E+$	$F+$	$A-$	$B-$
sequence code	$(9', 10')$	$(11', 12')$	$(13', 14')$	$(15', 16')$
slot serial number	$(17, \not{4})$	$(15, \not{2})$	$(13, \not{2}4)$	$(11, \not{2}2)$
phase bands	$C-$	$D-$	$E-$	$F-$
sequence code	$(17', 18')$	$(19', 20')$	$(21', 22')$	$(23', 24')$
slot serial number	$(9, \not{2}0)$	$(7, \not{1}8)$	$(5, \not{1}6)$	$(3, \not{1}4)$

[a]Slot serial number represents the upper-side position.

Table 6 Single-layer winding with $m = 3$, $Q = 18$, $2p = 4$

Phase bands	A	B	C
upper sides	(2, 11, 1)	(5, 14, 13)	(8, 17, 7)
lower sides	(6, 15, 4)	(9, 18, 16)	(12, 3, 10)

For the 22p20s-DL, the number of coils in each phase per cycle $Q/mt = 4$. Thus, there are two upper-side voltage phasors in each positive and negative phase bands per cycle. Then, the phase-band order of $m = 5$ is $A+$, $D-$, $B+$, $E-$, $C+$, $A-$, $D+$, $B-$, $E+$, and $C-$. According to (2), the sequence code i' can be converted to the slot serial number j

$$j = \frac{i' - 1 + 20k}{11} + 1$$

where k takes an integer that makes j be an integer, and $1 \le j \le 20$.

Then, the sequence code and the slot serial number are shown in Table 4. Moreover, the diagram of this winding distribution is shown in Fig. 3*b*.

For the 22p24s-SL, this winding can be regarded as a symmetric six-phase single-layer winding and satisfies the sufficient and necessary conditions $Q/4mt = 1$. For the purpose of a fast winding distribution, there are two main steps:

- Finish the whole process of the corresponding double-layer winding distributions.
- Remove even-numbered slot serial number.

For this corresponding double-layer winding, the number of coils in each phase per cycle $Q/mt = 4$. According to (5), there are two upper-side voltage phasors in each positive and negative phase bands per cycle. Then, the sequence code and the slot serial number can be determined in Table 5. Moreover, the diagram of this winding distribution is shown in Fig. 3*c*.

Finally, for this dual three-phase asymmetrical winding, select phases A, C, and E as 1 three-phase winding, and phases B, D, and F belong to the other.

For the 4p18s-SL, the distribution result of this corresponding double-layer winding is shown in Table 3. Then, let these coil sides in Table 3 be divided into upper and lower sides. This process has been introduced in detail in the previous analysis (when $a = b + 1$) and the result is shown in Table 6. It should be noted that there are two different types of coil pitch $y_q = 3$ and $y_q = 4$. Finally, the diagram of this winding distribution is shown in Fig. 3*d*.

2.4 Application: fast automatic winding distributions

Although conventional methods or some commercial software can also deal with automatic winding distributions, this process is tedious and time-consuming. The process of automatic winding distributions proposed in this subsection is fully based on the theory of symmetric winding distributions and has two obvious advantages:

- Thanks to Table 1, it is easy to obtain the feasibility of windings.
- Thanks to the winding distribution formula (2), the process of determining which phase each coil belongs to is much easier and faster than conventional methods.

The specific implementation for automatic winding distributions is:

- First, the values of m, Q, p, y_q, and winding type are given by the designer. Then, the feasibility of the windings can be obtained according to Table 1. If the winding is feasible, then go to the next step. Otherwise, re-define the values of m, Q, p, y_q, and winding type.
- Then, the order of phase bands is determined automatically and the number of upper sides q in each phase per cycle is calculated.
- Subsequently, the sequence code i' is obtained and the upper-side slot serial number j is obtained by (2).
- Finally, there are three different cases for winding distributions, a double-layer winding, a single-layer winding with a constant odd coil pitch and a single-layer winding with a non-odd coil pitch. For the first case, the upper-side slot serial number j has been obtained in the previous step. Then, the lower-side slot serial number is determined by the coil pitch y_q. For the second case, finish the whole process of the corresponding double-layer winding distributions and remove the even-numbered slot serial number. For the third case, let all coil sides be divided into upper and lower sides directly, which has been introduced in detail in the previous analysis.

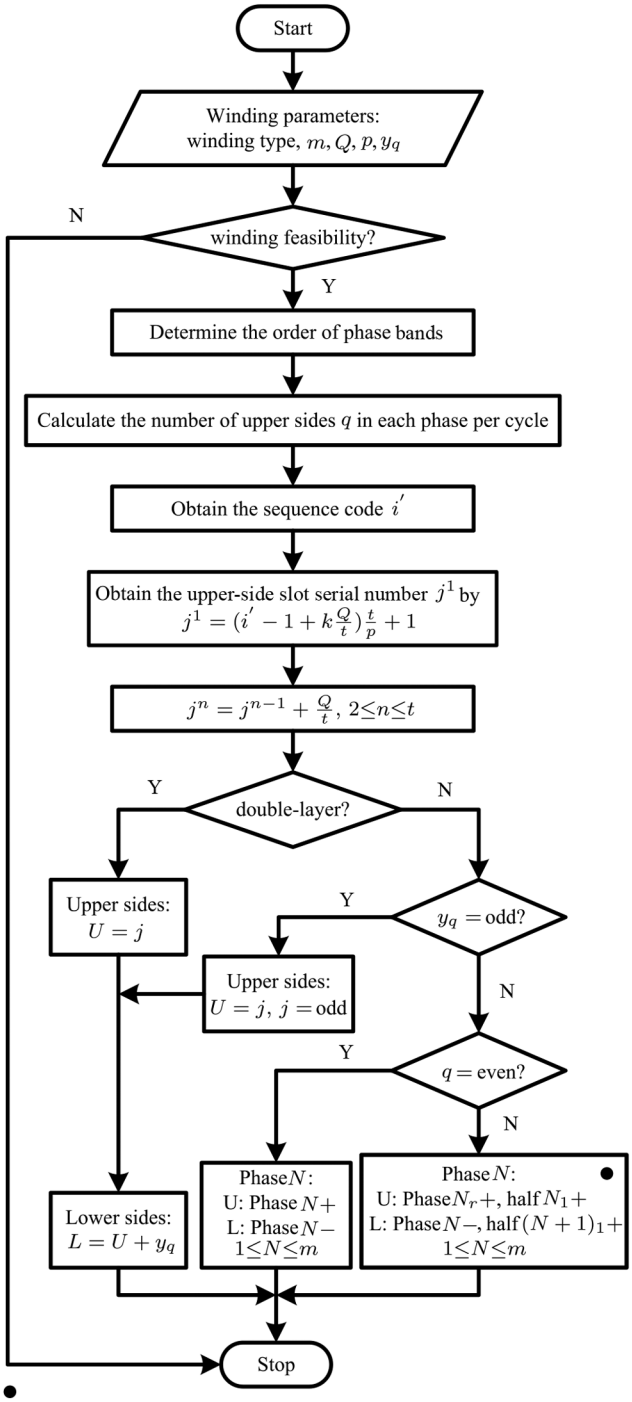

Fig. 4 *Flowchart of fast automatic winding distributions*

Subsequently, the flowchart of fast automatic winding distributions is shown in Fig. 4, which is also the algorithm for achieving automatic winding distributions by the computer program.

3 MMF calculation

In this section, a general MMF calculation method for double-layer windings with a constant coil pitch and single-layer windings with a constant odd coil pitch is proposed.

Before calculation, it is necessary to analyse the physical meaning of the number of basic windings t. Intuitively, the number of basic windings represents numbers for repetition of basic windings on the stator. Thus, the wavelength of the lowest sub-harmonic of the winding MMF waveform is $2\pi/t$. Then, it is necessary to define the magnetic angle x^{m}, which is shown as

$$x^{\mathrm{m}} = x^{\mathrm{mec}} \cdot t \tag{8}$$

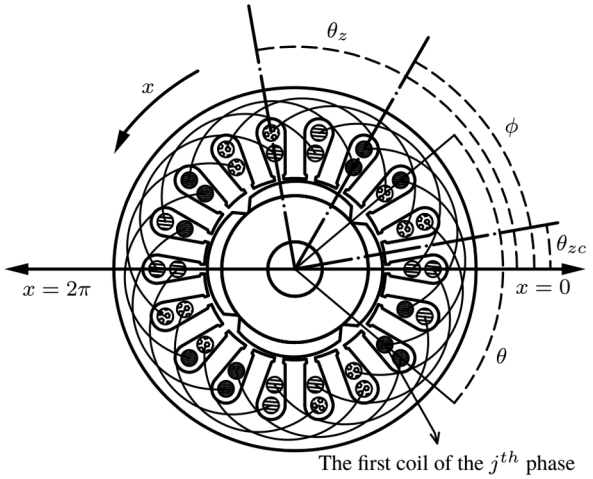

Fig. 5 *Coordinate system of MMF calculation*

where x^{m} is the magnetic angle, x^{mec} is mechanical angle and $t = \mathrm{GCD}(Q, p)$ for double-layer windings with a constant coil pitch, $t = \mathrm{GCD}(Q/2, p)$ for single-layer windings with a constant odd coil pitch.

Moreover, it should be noted that all angles in the MMF calculation are magnetic angles.

Then, the entire calculation process includes:

- Calculate the amplitude $\| f_{cv} \|$ of the MMF phasor in the vth-order harmonic for a single coil.
- Calculate the winding factor $k_{\mathrm{w}v}$ of the vth MMF, including pitch factor $k_{\mathrm{p}v}$ and distribution factor $k_{\mathrm{d}v}$.
- Determine the phase angle θ_z of the synthetic fundamental MMF phasor belonging to the jth phase.
- Calculate the spatial displacement ϕ between two adjacent phases.

Then, set $x = 0$ at the axis position of the first coil belonging to the jth phase, which is shown in Fig. 5.

According to the coordinate system in Fig. 5, the jth-phase MMF can be expressed as the following Fourier series expansion, which is shown as:

$$F_j = \sum_{v=1}^{\infty} \| f_{jv} \| \cdot k_{\mathrm{w}v} \cdot \cos(v(x + \theta_z - (j-1) \cdot \phi)) \tag{9}$$

where $\| f_{jv} \| = (\| f_{cv} \| / k_{\mathrm{p}v}) \cdot q$, here q is the number of coils in the jth phase per cycle, and $1 \le j \le m$, here m is the number of phases.

As mentioned in the previous section, since single-layer windings with a constant odd coil pitch can be fully converted to double-layer windings, the entire calculation process is almost the same for double-layer and single-layer windings. Thus, only the MMF calculation process for double-layer windings with a constant coil pitch is given in detail.

3.1 MMF calculation process for double-layer windings with a constant coil pitch

3.1.1 Calculate $\| f_{jv} \|$*:* For a single coil, its MMF waveform is a square wave when neglecting the effect of stator slots and the saturation of ferromagnetic material. Then, for a single coil, the amplitude $\| f_{cv} \|$ of the MMF phasor and pitch factor $k_{\mathrm{p}v}$ in the vth-order harmonics can be obtained by calculating its Fourier series, which are shown as

$$\| f_{cv} \| = \frac{2N_{\mathrm{c}} i_{\mathrm{c}} \cdot k_{\mathrm{p}v}}{v\pi}, \quad k_{\mathrm{p}v} = \sin\frac{v\theta}{2} \tag{10}$$

where θ is the coil span angle, which is shown in Fig. 5, i_c is coil current and N_c is coil turns.

Then, assume that I_j, N, and a_p are the jth-phase current, turns-in-series per phase and parallel branches, respectively. Thus, $\| f_{jv} \|$ can be written as:

$$\| f_{jv} \| = \frac{2NI_j}{v\pi t}, \quad I_j = i_c a_p, \quad N = \frac{qN_c}{a_p} \cdot t \tag{11}$$

where q is the number of coils in the jth phase per cycle and $q = Q/mt$ for double-layer windings with a constant coil pitch.

3.1.2 Calculate the distribution factor k_d*:* The key point when calculating the distribution factor k_d is to determine the spatial position of each coil, which is belonging to the jth phase.

Then, according to (2), the difference δ_0 between slot serial number of two adjacent upper sides, belonging to the positive phase $J+$ can be written as

$$\delta_0 = \left(1 + k_0 \frac{Q}{t}\right)\frac{t}{p} \tag{12}$$

where δ_0 and k_0 are integers.

Thus, the position angle α_1 between two adjacent coils in $J+$ or $J-$ can be expressed as $\delta_0\alpha^t$. For the vth MMF, this angle is $v\alpha_1$. Then, calculate the difference δ_1 between the slot serial number of the first upper side in $J+$ and the first one in $J-$. The sequence code of the first upper side in $J-$ depends on the parity of Q/mt.

When Q/mt is odd, the sequence code of the first upper side in $J-$ is $((Q+t)/2t)+1$. Then, δ_1 can be written as

$$\delta_1 = \left(\frac{Q+t}{2t} + k_1 \frac{Q}{t}\right)\frac{t}{p} \tag{13}$$

where δ_1 and k_1 are integers.

It can be proven that there must be an odd k_0 that lets δ_0 be even. Let $k_1 = (k_0 - 1)/2$, then $\delta_1 = \delta_0/2$. Thus, for the vth MMF, the position angle between the first upper sides in $J+$ and $J-$ is $v\alpha_1/2$. Since the current for coils in $J+$ and $J-$ has the same amplitude and opposite direction, the angle between the vth MMF phasors of the first coils in $J+$ and $J-$ is $(v\alpha_1/2)+\pi$.

When Q/mt is even, the sequence code of the first upper side in $J-$ is $(Q/2t)+1$. Then, δ_1 can be written as

$$\delta_1 = \left(\frac{Q}{2t} + k_1 \frac{Q}{t}\right)\frac{t}{p} \tag{14}$$

where δ_1 and k_1 are integers.

It is obvious that p/t must be odd. Let $k_1 = (p/2t) - (1/2)$, then $\delta_1 = Q/2t$. Thus, the angle between the vth MMF phasors of the first coils in $J+$ and $J-$ is $v\pi + \pi$.

Moreover, the distribution of the vth MMF phasors for each coil in the jth phase is shown in Fig. 6.

According to Fig. 6, the distribution factor k_d can be obtained:

$$k_d = \frac{\cos((q/4)\cdot v\alpha_1)}{q\cdot\cos(v\alpha_1/4)}, \quad \text{in Fig. 6}a$$

$$k_d = 0, \quad \text{in Fig. 6}b$$

$$k_d = \frac{\sin((q/4)\cdot v\alpha_1)}{(q/2)\cdot\cos(v\alpha_1/2)}, \quad \text{in Fig. 6}c$$

3.1.3 Calculate the phase angle θ_z *and the spatial displacement* ϕ*:* For the vth MMF, the equivalent MMF phasor $\dot{f}$ of all coils in J can be written as

$$\dot{f} = \| f_{jv} \| \cdot k_{wv} \cdot e^{j(v\alpha_1(a-1)/2)} \tag{15}$$

where a is the number of coils in $J+$ per cycle.

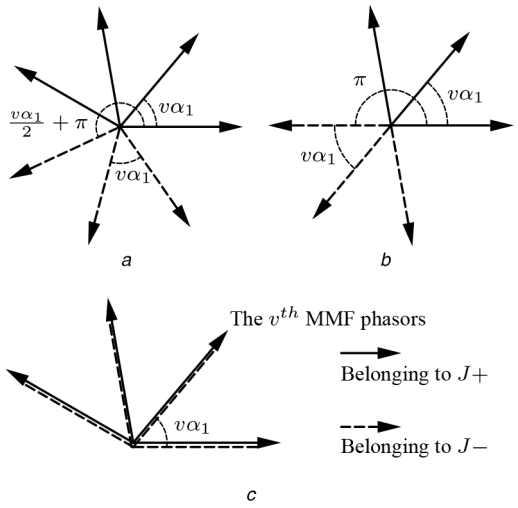

Fig. 6 *Distribution of the vth MMF phasors*
(a) *Q/mt* is odd, ***(b)*** *Q/mt* and *v* are even, ***(c)*** *Q/mt* is even and *v* is odd

Thus, according to (15), the phase angle θ_z of the synthetic fundamental MMF phasor belonging to the jth phase is $\alpha_1(a-1)/2$. It is worth pointing out that the relationship between the equivalent axis position θ_{zc} of the phase J shown in Fig. 5 and θ_z is that:

$$\theta_z = \theta_{zc} + k\pi$$

where k might be zero or one for double-layer windings with a constant coil pitch.

For the spatial displacement ϕ between two adjacent phases, calculate the difference Δ_ϕ of the slot serial number of the first upper sides in two adjacent phases, first. The sequence code of the first upper side in the phase $(J+1)+$ depends on the parity of m.

When m is odd, the sequence code of the first upper side in the phase $(J+1)+$ is $(Q/mt)+1$. Then, Δ_ϕ can be written as

$$\begin{aligned}\Delta_\phi &= \left(\frac{Q}{mt} + k_z\frac{Q}{t}\right)\frac{t}{p} \\ &= \frac{Q}{mt}\cdot(mk_z+1)\frac{t}{p} = \frac{Q}{mt}\cdot n\end{aligned} \tag{16}$$

where Δ_ϕ, k_z, and n are integers. Thus, the spatial displacement ϕ is $(2\pi n/m)(\Delta_\phi\alpha^t)$.

When m is even, the sequence code of the first upper side in the phase $(J+1)+$ is $(Q/2mt)+1$. Then, Δ_ϕ can be written as

$$\Delta_\phi = \left(\frac{Q}{2mt} + k_z\frac{Q}{t}\right)\frac{t}{p} = \frac{Q}{2mt}\cdot n \tag{17}$$

where Δ_ϕ, k_z, and n are integers. Thus, the spatial displacement ϕ is $\pi n/m$.

3.2 Summary

The calculation results of $\| f_{jv} \|$, k_{pv}, k_{dv}, θ_z, and ϕ for both double-layer windings with a constant coil pitch and single-layer windings with a constant odd coil pitch are all shown in Tables 9 and 10. It should be noted that the main harmonic order of MMF is $v = p/t$, which interacts with permanent-magnet flux linkage to product average torque.

Moreover, when $t = p$, this winding type is very common in motor design. Thus, the simplified calculation results of this winding type are also shown in Tables 11 and 12.

3.3 Validation of MMF calculation results

Table 7 shows the geometric parameters and excitation of the four models. Fig. 7 shows the geometric model of 4p18s-DL used in finite element analysis (FEA) calculation. It is noteworthy that the

Table 7 Geometric parameters and excitation of four models

Models	4p18s-DL	22p20s-DL	22p24s-SL	4p18s-SL
outer diameter of the stator		100 mm		
inner diameter of the stator		50 mm		
air-gap length		0.8 mm		
lamination length		100 mm		
slot type		closed slot		
number of turns per coil		10		
number of parallel branches		1		
current (DC), A	$I_a = 10$ $I_b = -5$ $I_c = -5$	$I_a = 10$ $I_b = -2.5$ $I_c = -2.5$ $I_d = -2.5$ $I_e = -2.5$	$I_a = 10$ $I_b = -5$ $I_c = -5$ $I_d = 10$ $I_e = -5$ $I_f = -5$	$I_a = 10$ $I_b = -5$ $I_c = -5$

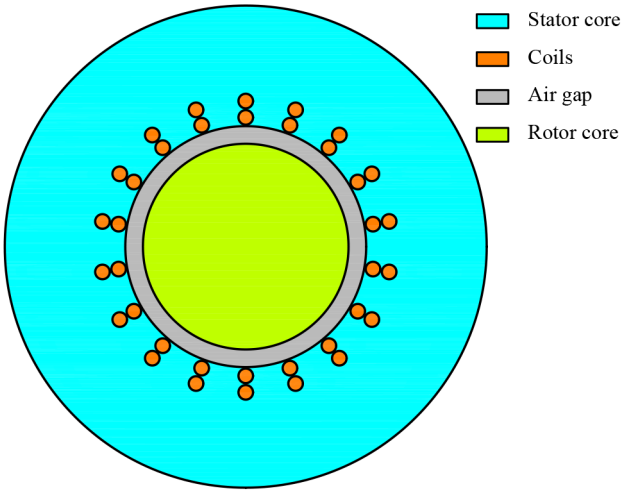

Fig. 7 *Geometric model of 4p18s-DL used in FEA calculation*

Table 8 Pitch, distribution, and winding factors of four models

Models	4p18s-DL			22p20s-DL			22p24s-SL			4p18s-SL		
v	k_{pv}	k_{dv}	k_{wv}	k_{pv}	k_{dv}	k_{wv}	k_{pv}	k_{dv}	k_{wv}	k_{pv_1}	k_{pv_2}	k_{wv}
1	**0.985**	**−0.960**	**−0.945**	0.156	−0.156	−0.024	0.131	1.000	0.131	0.500	0.643	0.167
2	0.342	0.177	0.061	0.309	0.000	0.000	0.259	0.000	0.000	**0.866**	**0.985**	**0.897**
3	−0.866	−0.667	0.577	0.454	0.454	0.206	0.383	1.000	0.383	1.000	0.866	0.333
4	−0.643	−0.218	0.140	0.588	0.000	0.000	0.500	0.000	0.000	0.866	0.342	0.398
5	0.643	−0.218	−0.140	0.707	−0.707	−0.500	0.609	1.000	0.609	0.500	−0.342	0.167
6	0.866	−0.667	−0.577	0.809	0.000	0.000	0.707	0.000	0.000	0.000	−0.866	0.577
7	−0.342	0.177	−0.061	0.891	0.891	0.794	0.793	1.000	0.793	−0.500	−0.985	0.167
8	−0.985	−0.960	0.945	0.951	0.000	0.000	0.866	0.000	0.000	−0.866	−0.643	0.186
9	−0.000	0.333	−0.000	0.988	−0.988	−0.976	0.924	1.000	0.924	−1.000	−0.000	0.333
10	0.985	−0.960	−0.945	1.000	0.000	0.000	0.966	0.000	0.000	−0.866	0.643	0.707
11	0.342	0.177	0.061	**0.988**	**0.988**	**0.976**	**0.991**	**1.000**	**0.991**	−0.500	0.985	0.167

Bold values indicate main harmonic in four models.

four models have the same geometric models except the winding configuration, therefore in Fig. 7 only the 4p18s-DL is given as an example.

Then, the calculated pitch, distribution and winding factors for the four models from the proposed theory are shown in Table 8.

Moreover, for the winding factors of various harmonics, an open-source program Koil [23] is used to validate the analytical calculation, their comparisons are shown in Fig. 8, where the analytical calculation results are denoted as AM. Note that the Koil program cannot deal with the 4p18s-SL winding structure. Further, the main harmonic order of MMF is $v = p/t$. Thus, the first order is main harmonic in the 4p18s-DL. The second order is the main harmonic in the 4p18s-SL. The 11th order is the main harmonic in the 22p20s-DL and the 22p24s-SL. Clearly, the calculation results based on the proposed theory are exactly the same as the results from Koil.

Figs. 9 and 10 show the winding MMF waveform and the harmonics spectrum of the four models from analytical calculation results and Koil results. It can be seen that the calculation results from the proposed theory agree well with the Koil results.

In the Section 3.1, the expression of the jth-phase MMF has been obtained. Thus, the whole MMF of the m-phase winding can be expressed as

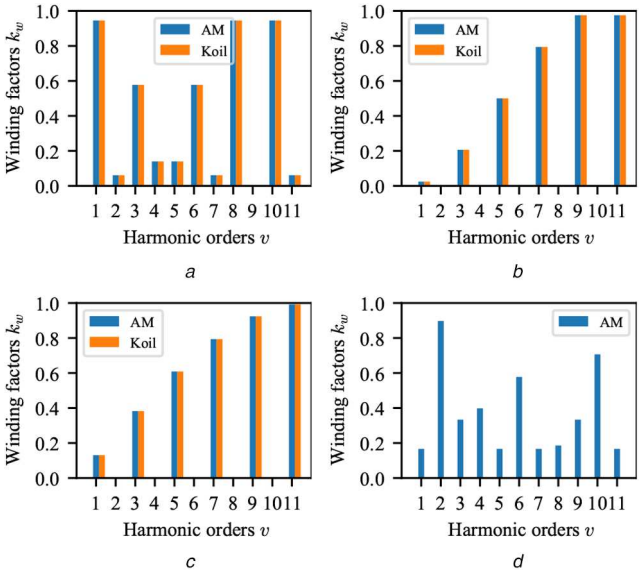

Fig. 8 *Validation of winding factors*
(a) 4p18s-DL, ***(b)*** 22p20s-DL, ***(c)*** 22p24s-SL, ***(d)*** 4p18s-SL

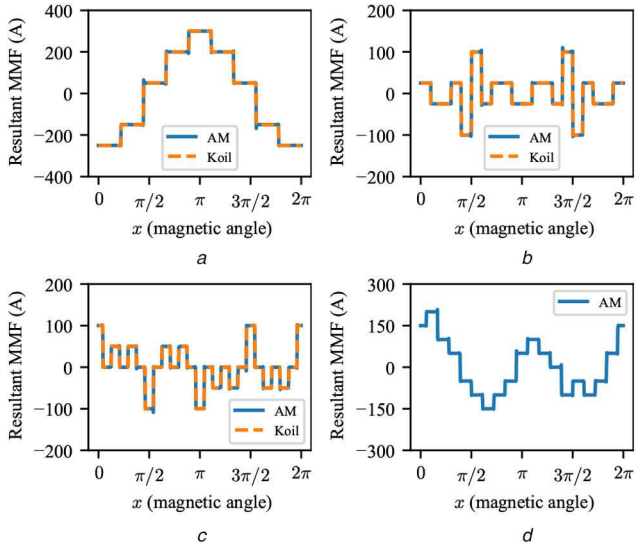

Fig. 9 *Validation of winding MMF waveform*
(a) 4p18s-DL, ***(b)*** 22p20s-DL, ***(c)*** 22p24s-SL, ***(d)*** 4p18s-SL

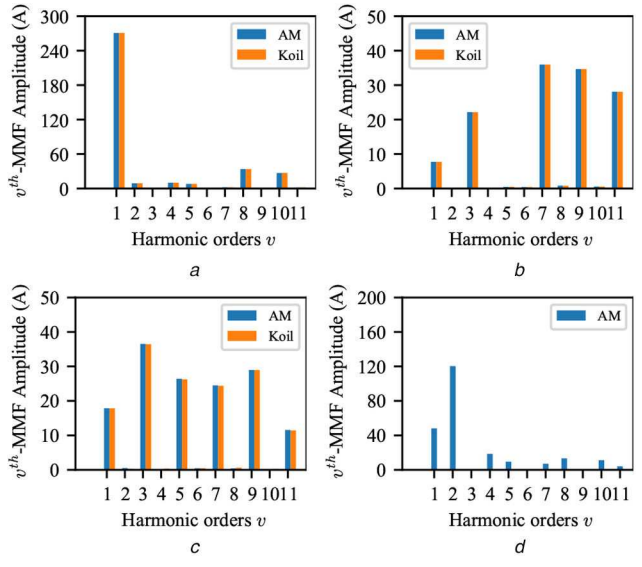

Fig. 10 *Validation of winding MMF harmonics spectrum*
(a) 4p18s-DL, ***(b)*** 22p20s-DL, ***(c)*** 22p24s-SL, ***(d)*** 4p18s-SL

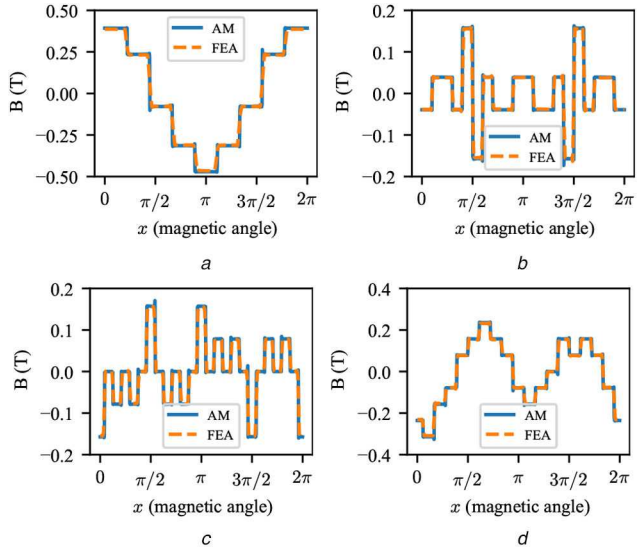

Fig. 11 *Validation of air-gap flux density waveform*
(a) 4p18s-DL, ***(b)*** 22p20s-DL, ***(c)*** 22p24s-SL, ***(d)*** 4p18s-SL

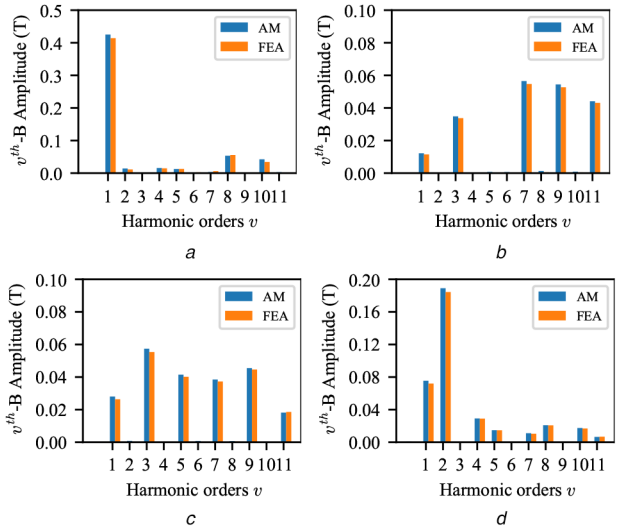

Fig. 12 *Validation of air-gap flux density harmonics spectrum*
(a) 4p18s-DL, ***(b)*** 22p20s-DL, ***(c)*** 22p24s-SL, ***(d)*** 4p18s-SL

$$F = \sum_{j=1}^{m} \sum_{v=1}^{\infty} \| f_{jv} \| \cdot k_{wv} \cdot \cos(v(x + \theta_z - (j-1) \cdot \phi)) = \sum_{j=1}^{m} F_j \tag{18}$$

The air-gap flux density B_g can be calculated by using FEM and can be compared with the analytical result by

$$B_g^{AM} = \frac{-\mu_0 \sum_{j=1}^{m} F_j}{g} \tag{19}$$

where the air-gap length g is constant and μ_0 is the air permeability.

To verify the accuracy of the air-gap flux density B_g^{AM} from (19), Figs. 11 and 12 show the air-gap flux density waveform and harmonics spectrum of the four models from the analytical calculation results and FEA results. From Figs. 11 and 12, it can be seen that air-gap flux density B_g^{AM} from (19) is accurate when neglecting the effect of stator slots and the saturation of ferromagnetic material. From Figs. 11*a* and *d*, it can also be seen that the amplitude of positive and negative half-wave is asymmetrical in the air-gap density waveform, which is caused by the even-numbered harmonics existing in the winding MMF.

4 Conclusion

This paper presents a unified theory of the symmetric winding distributions and a general method for symmetric winding MMF harmonic analysis. This theory can be used in general winding design and some important conclusions are shown as follows.

- Table 1 gives criteria for the feasible arbitrary winding with m-phase, the number of slots Q and pole pairs p directly.
- A novel winding distribution formula (2) establishes the relationship between the sequence code and the slot serial number, which is applied in automatic winding distributions.
- The winding MMF harmonics including the amplitude of MMF harmonics and harmonic orders are presented in Tables 9–12, which are shown in Appendix.

5 Acknowledgments

This work was supported by the Natural Science Foundation of China under the grant nos. 51837010 and 51690182.

6 References

[1] El-Refaie, A.M.: 'Fractional-slot concentrated-windings synchronous permanent magnet machines: opportunities and challenges', *IEEE Trans. Ind. Electron.*, 2009, **57**, (1), pp. 107–121

[2] Li, J., Choi, D.W., Son, D.H., *et al.*: 'Effects of MMF harmonics on rotor eddy-current losses for inner-rotor fractional slot axial flux permanent magnet synchronous machines', *IEEE Trans. Magn.*, 2012, **48**, (2), pp. 839–842

[3] Cros, J., Viarouge, P.: 'Synthesis of high performance PM motors with concentrated windings', *IEEE Trans. Energy Convers*, 2002, **17**, (2), pp. 248–253

[4] Jack, A.G., Mecrow, B.C., Haylock, J.A.: 'A comparative study of permanent magnet and switched reluctance motors for high-performance fault-tolerant applications', *IEEE Trans. Ind. Appl.*, 1996, **32**, (4), pp. 889–895

[5] Mecrow, B.C., Jack, A.G., Atkinson, D.J., *et al.*: 'Design and testing of a four-phase fault-tolerant permanent-magnet machine for an engine fuel pump', *IEEE Trans. Energy Convers*, 2004, **19**, (4), pp. 671–678

[6] Rao, J., Gao, Y., Li, D., *et al.*: 'Performance analysis of interior permanent magnet motor using overlapping windings with fractional ratio of slot to pole pair', *IEEE Trans. Appl. Supercond.*, 2016, **26**, (7), pp. 1–5

[7] Tang, N., Brown, I.P.: 'Family phenomenon in electric machine winding MMF space harmonics: attribution and applications', *IEEE Trans. Magn.*, 2019, **55**, (5), pp. 1–10

[8] Dajaku, G., Xie, W., Gerling, D.: 'Reduction of low space harmonics for the fractional slot concentrated windings using a novel stator design', *IEEE Trans. Magn.*, 2013, **50**, (5), pp. 1–12

[9] Liwschitz-Garik, M., Whipple, C.C.: '*Alternating-current machines*' (van Nostrand, USA, 1961)

[10] Bianchi, N., Pre, M.D.: 'Use of the star of slots in designing fractional-slot single-layer synchronous motors', *IEE Proc. Electr. Power Appl.*, 2006, **153**, (3), pp. 459–466

[11] Bianchi, N., Bolognani, S., Pre, M.D., *et al.*: 'Design considerations for fractional-slot winding configurations of synchronous machines', *IEEE Trans. Ind. Appl.*, 2006, **42**, (4), pp. 997–1006

[12] Barcaro, M., Bianchi, N., Magnussen, F.: 'Six-phase supply feasibility using a PM fractional-slot dual winding machine', *IEEE Trans. Ind. Appl.*, 2010, **47**, (5), pp. 2042–2050

[13] Abdel-Khalik, A.S., Ahmed, S., Massoud, A.M.: 'Low space harmonics cancelation in double-layer fractional slot winding using dual multiphase winding', *IEEE Trans. Magn.*, 2015, **51**, (5), pp. 1–10

[14] Bianchi, N., Bolognani, S., Bon, D., *et al.*: 'Torque harmonic compensation in a synchronous reluctance motor', *IEEE Trans. Energy Convers*, 2008, **23**, (2), pp. 466–473

[15] Han, S.H., Jahns, T.M., Soong, W.L., *et al.*: 'Torque ripple reduction in interior permanent magnet synchronous machines using stators with odd number of slots per pole pair', *IEEE Trans. Energy Convers*, 2010, **25**, (1), pp. 118–127

[16] Sun, A., Li, J., Qu, R., *et al.*: 'Effect of multilayer windings on rotor losses of interior permanent magnet generator with fractional-slot concentrated-windings', *IEEE Trans. Magn.*, 2014, **50**, (11), pp. 1–4

[17] Bianchi, N., Fornasiero, E.: 'Impact of MMF space harmonic on rotor losses in fractional-slot permanent-magnet machines', *IEEE Trans. Energy Convers*, 2009, **24**, (2), pp. 323–328

[18] Gundogdu, T., Komurgoz, G.: 'Investigation of winding MMF harmonic reduction methods in IPM machines equipped with FSCWs', *Int. Trans. Electr. Energy*, 2019, **29**, (1), pp. e2688.1–e2688.27

[19] Dajaku, G., Gerling, D.: 'The influence of permeance effect on the magnetic radial forces of permanent magnet synchronous machines', *IEEE Trans. Magn.*, 2013, **49**, (6), pp. 2953–2966

[20] Wu, L.J., Zhu, Z.Q., Chen, J.T., *et al.*: 'An analytical model of unbalanced magnetic force in fractional-slot surface-mounted permanent magnet machines', *IEEE Trans. Magn.*, 2010, **46**, (7), pp. 2686–2700

[21] El-Refaie, A.M., Shah, M.R., Qu, R., *et al.*: 'Effect of number of phases on losses in conducting sleeves of surface PM machine rotors equipped with fractional-slot concentrated windings', *IEEE Trans. Ind. Appl.*, 2008, **44**, (5), pp. 1522–1532

[22] Gundogdu, T.: '*Advanced non-overlapping winding induction machines for electrical vehicle applications*' (University of Sheffield, UK, 2018)

[23] Alberti, L.: 'Koil: A tool to design the winding of rotating electric machinery'. Proc Int Conf on Electrical Machines (ICEM 2018), Alexandroupoli, Greece, 2018, pp. 805–811

7 Appendix

The MMF calculation parameters for a general winding are presented in Tables 9–12.

Table 9 MMF parameters for double-layer windings with a constant coil pitch

$\left(m, \frac{Q}{mt}\right)$	$\| f_{jv} \|$	k_{pv}	k_{dv}	θ_z	ϕ
(odd, odd)[a]	$\frac{2NI_j}{v\pi t}$	$\sin\frac{v\theta}{2}$	$\frac{\cos((Q/4mt)\cdot v\alpha_1)}{(Q/mt)\cdot\cos(v\alpha_1/4)}$	$\frac{\alpha_1(a-1)}{2}$	$\frac{2\pi n}{m}$
(odd, even)[b]			$\begin{cases} 0 & v=\text{even} \\ \frac{\sin((Q/4mt)\cdot v\alpha_1)}{(Q/2mt)\cdot\sin(v\alpha_1/2)} & v=\text{odd} \end{cases}$		$\frac{\pi n}{m}$
(even, even)[c]					

$I_j = i_c a_p$, $N = (N_c/a_p)\cdot(Q/m)$, here i_c, a_p, and N_c are coil current, coil turns and parallel branches, respectively; $\theta = y_q\alpha^t$, $\alpha^t = 2\pi t/Q$, and $t = \text{GCD}(Q, p)$.

[a] $\alpha_1 = (\alpha^t + 2k_0\pi)\cdot(t/p)$, here k_0 takes a positive odd integer that makes $(1 + k_0\cdot(Q/t))\cdot(t/p)$ be even; $a = (Q/2mt) + (1/2)$; k_z takes an integer that makes $n = (mk_z + 1)/(p/t)$ be an integer.

[b] n is the same as 1; $\alpha_1 = (\alpha^t + 2k_0\pi)\cdot(t/p)$, here k_0 takes an integer that makes $(1 + k_0\cdot(Q/t))\cdot(t/p)$ be an integer; $a = Q/2mt$.

[c] α_1 is the same as 2; k_z takes an integer that makes $n = (2mk_z + 1)/(p/t)$ be an integer.

Table 10 MMF parameters for single-layer windings with a constant odd coil pitch

$\left(m, \frac{Q}{mt}, \frac{Q}{2mt}\right)$	$\| f_{jv} \|$	k_{pv}	k_{dv}	θ_z	ϕ
(odd, odd,/)[a]	$\frac{4NI_j}{v\pi t}$	$\sin\frac{v\theta}{2}$	$\frac{\cos((Q/4mt)\cdot v\alpha_1)}{(Q/mt)\cdot\cos(v\alpha_1/4)}$	$\frac{\alpha_1(a-1)}{2}$	$\frac{2\pi n}{m}$
(odd, even, odd)[b]	$\frac{2NI_j}{v\pi t}$		$\frac{\cos((Q/8mt)\cdot v\alpha_1)}{(Q/2mt)\cdot\cos(v\alpha_1/4)}$		
(odd, even, even)[c]			$\begin{cases} 0 & v=\text{even} \\ \frac{\sin((Q/8mt)\cdot v\alpha_1)}{(Q/4mt)\cdot\sin(v\alpha_1/2)} & v=\text{odd} \end{cases}$		$\frac{\pi n}{m}$
(even, even, even)[d]					

$I_j = i_c a_p$, $N = (N_c/a_p)\cdot(Q/2m)$, here i_c, a_p, and N_c are coil current, parallel branches, and coil turns, respectively; $\alpha^t = 2\pi t/Q$, $t = \text{GCD}(Q, p)$.

[a] $\theta = y_q\alpha^t/2$; $\alpha_1 = (\alpha^t + 2k_0\pi)\cdot(t/2p)$, here k_0 takes a positive odd integer that makes $(1 + k_0\cdot(Q/t))\cdot(t/2p)$ be even; $a = (Q/2mt) + (1/2)$; k_z takes an integer that makes $n = (mk_z + 1)/(2p/t)$ be an integer.

[b] $\theta = y_q\alpha^t$; $\alpha_1 = (2\alpha^t + 2k_0\pi)\cdot(t/p)$, here k_0 takes a positive odd integer that makes $(1 + k_0\cdot(Q/2t))\cdot(t/p)$ be even; $a = (Q/4mt) + (1/2)$; k_z takes an integer that makes $n = (mk_z + 1)/(p/t)$ be an integer.

[c] θ and n are the same as b; $\alpha_1 = (2\alpha^t + 2k_0\pi)\cdot(t/p)$, here k_0 takes an integer that makes $(1 + k_0\cdot(Q/2t))\cdot(t/p)$ be an integer; $a = Q/4mt$.

[d] θ, α_1, and a are the same as c; k_z takes an integer that makes $n = (2mk_z + 1)/(p/t)$ be an integer.

Table 11 MMF parameters for double-layer windings with a constant coil pitch when $t = p$

$\left(m, \frac{Q}{mp}\right)$	$\| f_{jv} \|$	k_{pv}	k_{dv}	θ_z	ϕ
(odd, odd)	$\frac{2NI_j}{v\pi p}$	$\sin\frac{vy_q\alpha^e}{2}$	$\frac{\cos((v\pi/2m) + (Q/mp)\cdot(v\pi/2))}{(Q/mp)\cdot\cos((v\alpha^e/4) + (v\pi/2))}$	$\left(\frac{\alpha^e}{2} + \pi\right)\cdot\left(\frac{Q}{2mp} - \frac{1}{2}\right)$	$\frac{2\pi}{m}$
(odd, even)			$\begin{cases} 0 & v=\text{even} \\ \frac{\sin(v\pi/2m)}{(Q/2mp)\cdot\sin(v\alpha^e/2)} & v=\text{odd} \end{cases}$	$\frac{\alpha^e}{2}\cdot\left(\frac{Q}{2mp} - 1\right)$	
(even, even)					$\frac{\pi}{m}$

I_j and N are the same as those in Table 9; $\alpha^e = 2\pi p/Q$.

Table 12 MMF parameters for single-layer windings with a constant odd coil pitch when $t = p$

$\left(m, \frac{Q}{mp}, \frac{Q}{2mp}\right)$	$\| f_{jv} \|$	k_{pv}	k_{dv}	θ_z	ϕ
(odd, odd, /)[a]	$\frac{4NI_j}{v\pi p}$	$\sin\frac{vy_q\alpha^e}{4}$	$\frac{\cos((v\pi/4m) + (Q/mp)\cdot(kv\pi/4))}{(Q/mp)\cdot\cos((v\alpha^e/8) + (kv\pi/4))}$	$\left(\frac{\alpha^e}{4} + \frac{k\pi}{2}\right)\cdot\left(\frac{Q}{2mp} - \frac{1}{2}\right)$	$\frac{\pi}{m} + \pi$
(odd, even, odd)	$\frac{2NI_j}{v\pi p}$	$\sin\frac{vy_q\alpha^e}{2}$	$\frac{\cos((v\pi/2m) + (Q/2mp)\cdot(v\pi/2))}{(Q/2mp)\cdot\cos((v\alpha^e/2) + (v\pi/2))}$	$(\alpha^e + \pi)\cdot\left(\frac{Q}{4mp} - \frac{1}{2}\right)$	$\frac{2\pi}{m}$
(odd, even, even)			$\begin{cases} 0 & v=\text{even} \\ \frac{\sin(v\pi/2m)}{(Q/4mp)\cdot\sin(v\alpha^e)} & v=\text{odd} \end{cases}$	$\alpha^e\cdot\left(\frac{Q}{4mp} - 1\right)$	
(even, even, even)					$\frac{\pi}{m}$

[a] $k = (Q/p) + 2$; I_j and N are the same as those in Table 10; $\alpha^e = 2\pi p/Q$.